Available online at www.sciencedirect.com
SCIENCE DIRECT
Solid State Communications 137 (2006) 199–202
solid state communications
www.elsevier.com/locate/ssc

Preparation and optical properties of Ag enwrapped Y_2O_3:Eu^{3+} nanoparticles in solution and in powders

Zhongxin Liu [a,b], Hongwei Song [a,*], Ruifei Qin [a,b], Guohui Pan [a,b], Xue Bai [a,b]

[a] *Key Laboratory of Excited State Physics, Changchun Institute of Optics, Fine Mechanics and Physics, Chinese Academy of Sciences, 16 Eastern South-Lake Road, Changchun 130033, People's Republic of China*
[b] *Graduate School of Chinese Academy of Sciences, Beijing 10039, People's Republic of China*

Received 18 August 2005; received in revised form 8 November 2005; accepted 8 November 2005 by A. Pinczuk
Available online 28 November 2005

Abstract

Ag enwrapped Y_2O_3:Eu^{3+} nanoparticles were prepared by a wet chemistry method, which was dispersed in liquid (glycol) or dried to powders. Their luminescence properties were studied in comparison to those in the un-enwrapped ones. The results demonstrated that in glycol the $^5D_0$–$^7F_2$ transitions for Ag enwrapped Y_2O_3:Eu^{3+} nanoparticles became stronger than that for un-enwrapped ones, while the excitation charge transfer band shifted blue. On the contrary, the $^5D_0$–$^7F_2$ transitions in Ag enwrapped Y_2O_3:Eu^{3+} powders became weaker than those in the un-enwrapped ones. It was suggested that in liquid the Ag shells thinly deposited in the surface of Y_2O_3:Eu^{3+} and insulated the Y_2O_3:Eu^{3+} from the liquid, which contained large organic vibration modes. As a result, the surface nonradiative energy transfer from Eu^{3+} to the organic modes decreased, and emission intensity of $^5D_0$–$^7F_2$ increased. In the Y_2O_3:Eu^{3+} powders, the Ag shells absorbed the excitation light, leading to the decrease in excitation density and the intensity of $^5D_0$–$^7F_2$.

PACS: 78.55.Hx; 78.67.Bf; 81.20.Ka

Keywords: A. Nanostructures; B. Chemical synthesis; D. Optical properties; E. Luminescence

1. Introduction

Active research has been carried out in the optical properties of rare-earth ions in low-dimensional metal or semiconductors because of their potential application in optoelectronic devices [1–3] and biological luminescent labels [4–6]. Many rare-earth phosphors with the potential application in biological systems are extensive studied now [7–9]. In contrast to the traditional organic dyes, the advantages of the fluorescent nanocrystals are their high quantum efficiency, tunable emission wavelength, and high stability against photobleaching. How to improve the ability to sense the state of biological systems optically is a promising strategy that requires increasing more-intense signals from the emitting crystals in liquid state. Energy transfer is a useful method to enhance the luminescence common in use. Recently, metal nanoparticles gained considerable attention for their strong surface plasma resonance absorption at visible region, where correspond to the emission of rare-earth ions. It is considered that the luminescence enhancement of rare earths will be observed if a proper excitation wavelength is selected, in metal nanoparticle modified materials. In 1999, Hayakawa et al. [10–12] reported the luminescence enhancement from Eu^{3+} in the sol–gel glasses, which was attributed to the local field enhancement around Eu^{3+} induced by surface plasma oscillation of silver particles. Very recently, Perriat et al. reported [13] that in diethylene glycol the enwrapped gold nanoparticles caused the luminescence increase in Tb^{3+} in Tb_2O_3 nanoparticles. They considered that the luminescence enhancement of Tb^{3+} originated from the energy transfer between nanoscale Au and Tb_2O_3 nanoparticles. In despite of all the researches, the interaction between rare-earth and metal nanoparticles in different states is still uncertain, and their origin is unclear. In this paper, we reported in the glycol solution and in the Y_2O_3:Eu^{3+} powder, the influence of Ag enwrapping on the photoluminescence of Y_2O_3:Eu^{3+} nanoparticles.

* Corresponding author. Fax: +86 431 6176320.
E-mail address: hwsong2005@yahoo.com.cn (H. Song).

0038-1098/$ - see front matter © 2005 Elsevier Ltd. All rights reserved.
doi:10.1016/j.ssc.2005.11.019

2. Experiments

The preparation of the samples was finished in two steps. First, the nanopowders of Y_2O_3:Eu^{3+} were prepared by glycine-nitrate solution combustion synthesis [14]. The procedures are as follows: first, the Y_2O_3:Eu^{3+} and glycine with appropriate ratio ($G/N=1.45$) were dissolved by distilled water and nitric acid in a beaker. The M-nitrate, M $(NO_3)_n$, was also dissolved in distilled water in a beaker. Subsequently, the two solutions were mixed together. The molar ratio of Eu:Y for starting materials was controlled to be 0.05. Then, the mixed solution was gradually heated up until its excess free water evaporated and became sticky. The system self-combusted for a few seconds as it reached a certain temperature. As the reaction was finished, the resultant ashes were collected. The samples were calcined at 500 °C for 1 h to decompose the residual NO_3^-, and then white powders were gained. Second, the Y_2O_3:Eu^{3+} nanopowders (0.07 g) were sufficiently dispersed in glycol (20 mL) by ultrasonic, then $AgNO_3$ (0.01 g) were added to one of the solutions and maintained ultrasonic dispersion for another 2 h. After that, the mixture was heated to 100 °C in a flask for 30 min. In this process, the Ag was reduced and the color of the mixture was changed to brown. When the mixture centrifuged and washed with deionized water, the powder samples were gained. In order to estimate the size of the Ag nanoparticles, the Ag nanoparticles were prepared by the same procedure, without adding Y_2O_3:Eu^{3+} nanoparticles.

The morphology and structure of the particles were observed with a JEM-2010 transmission electron microscope made by Japanese JEOL Company. X-ray diffraction (XRD) data were collected on Rigaku D/max-rA X-ray diffractometer using a Cu target radiation source ($\lambda=1.54078$ Å). The energy-dispersive X-ray (EDX) was measured by Oxford ISIS-300 spectra. Excitation and emission spectra at room temperature were measured with a Hitachi F-4500 fluorescence spectrometer. In the measurements of fluorescence dynamics, a 266-nm light generated from the Fourth-Harmonic-Generator pumped by the pulsed Nd:YAG laser was used as excitation source. The Nd:YAG laser was with a line width of 1.0 cm^{-1}, pulse duration of 10 ns and repetition frequency of 10 Hz. A Spex-1403 spectrometer, a boxcar integrator and a computer were used as recording.

3. Results and discussion

Fig. 1 shows the TEM micrographs of the Y_2O_3:Eu^{3+} before and after enwrapped with Ag nanoparticles. For the limitation of combustion method, the size of the Y_2O_3:Eu^{3+} is not very equality. As shown in Fig. 1(a), the Y_2O_3:Eu^{3+} nanoparticles synthesized by the combustion method tended to agglomerate together. After enwrapped with Ag nanoparticles (Fig. 1(b)), the Y_2O_3:Eu^{3+} nanoparticles were well dispersed. In Fig. 1(c), it can be seen that a part of particle edge is faint, implying that some particles were not completely enwrapped by Ag nanoparticles. In Fig. 1(d), the whole particle edge is faint, suggesting that these Y_2O_3 spheres were perfectly

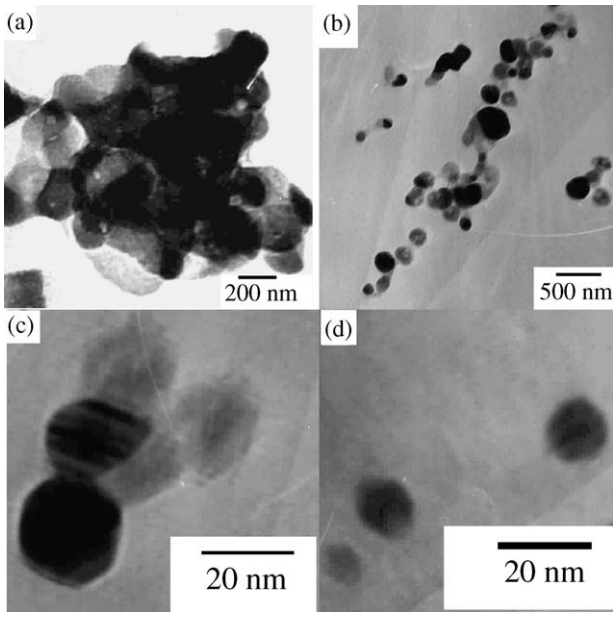

Fig. 1. TEM images of Y_2O_3:Eu^{3+}/Ag nanoparticles. ((a) Y_2O_3:Eu^{3+} un-enwrapped with Ag. (b) Y_2O_3:Eu^{3+} enwrapped with Ag nanoparticles. (c) The selected area TEM image of the imperfect enwrapped nanoparticles. (d) The selected area TEM image the perfect enwrapped nanoparticles).

enwrapped by Ag nanoparticles. Fig. 2 shows the TEM images of Ag nanoparticles prepared by the same method in glycol. It can be seen that the size of the Ag nanoparticles was about 3 nm. This suggested that the Ag nanoparticles enwrapped surrounding Y_2O_3 particles should be several nanometers.

Fig. 3(a) shows the XRD patterns of Y_2O_3:Eu^{3+} nanoparticles wrapped with Ag and not. In general, the nanocrystalline Y_2O_3 were cubic in symmetry. Substitution of Eu^{3+} ions for Y had no obvious influence on the cubic structure of Y_2O_3. Seen as the pattern, the presence of Ag was not influenced the crystal structure of Y_2O_3:Eu^{3+}. The diffraction peak originated from (111) of Ag was observed in the Ag wrapped Y_2O_3:Eu^{3+} EDX spectrum (Fig. 3(b)) shows that Ag was indeed exist in the powder sample and the content was about 2%.

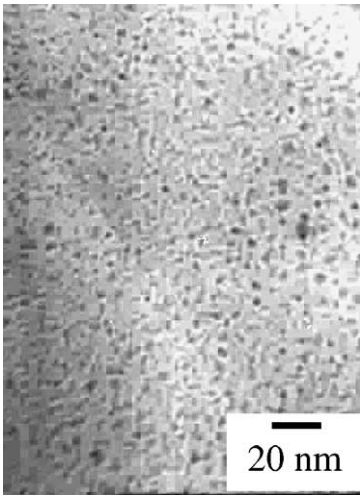

Fig. 2. TEM images of Ag nanoparticles.

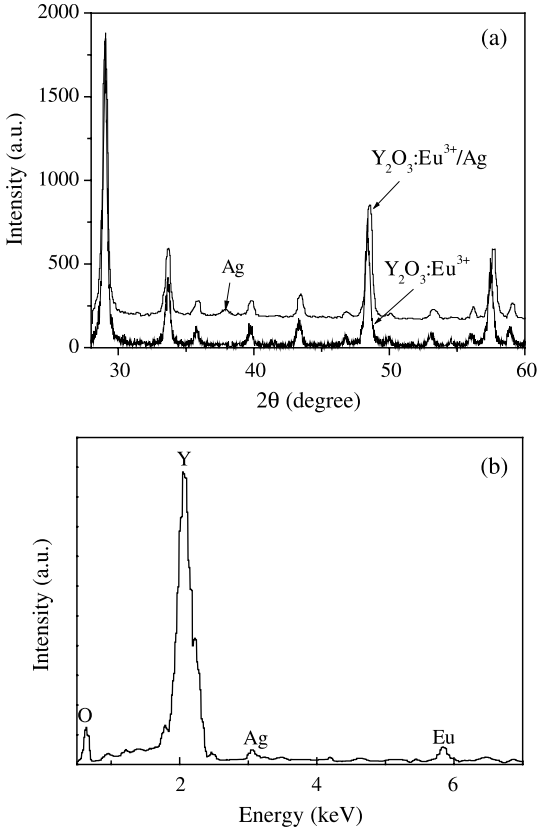

Fig. 3. (a) XRD patterns of the Y_2O_3:Eu^{3+} nanoparticles before and after enwrapped with Ag (b) EDX spectrum of Y_2O_3:Eu^{3+}/Ag nanoparticles in powder.

Fig. 4 shows the excitation spectra of Eu^{3+} in different samples. In all the spectra, the band extended from 220 to 300 nm was assigned to the charge transfer (CT) transition, which originated from the electronic transition from the 2p orbital of O^{2-} to the 4f orbital of Eu^{3+}. The sharp lines in the range of 300–590 nm are assigned to direct f–f transitions of Eu^{3+}. No plasma resonant absorption peak of Ag was observed, implying that there was no sufficient energy transfer from the Ag nanoparticles to Eu^{3+} ions. In the glycol solution (Fig. 4(a)), the CT band in Y_2O_3:Eu^{3+}/Ag was at ~ 250 nm, which was quite consistent with the literature [15] on cubic Y_2O_3:Eu^{3+} powders. The CT band for Y_2O_3:Eu^{3+} in the glycol solution red-shifted to ~266 nm.

The CT band of Y_2O_3:Eu^{3+} is related closely to the covalency between O^{2-} and Eu^{3+} and coordination environment around Eu^{3+}. In the solution, the surface coordination environment surrounding Eu^{3+} ions was changed largely. The red-shift of CT band represents the increase in the covalency, the decrease in ionicity between oxygen and Eu^{3+}. In the powders (Fig. 4(b)), the location of CT transition did not shift before and after enwrapping. In addition, the band associated with the exciton transition of the Y_2O_3 host lattice [16] was observed nearby 210 nm. It was also seen that in the glycol solution, the intensity of the CT transition for the Ag wrapped sample increased several times than that for the un-wrapped one. On the contrary, in Ag wrapped Y_2O_3:Eu^{3+} powders, the intensity of the CT excitation transitions decreased than that in the un-wrapped one. This result was well in consistent with the results of emission spectra, as shown in Fig. 5.

The fluorescence dynamics for the $^5D_0$–$^7F_2$ transitions of Eu^{3+} in the powder samples were also studied. The results demonstrated that in both Ag-wrapped and un-wrapped samples, the $^5D_0$–$^7F_2$ transitions decayed exponentially. The exponential fluorescence lifetimes were determined to be 1.56 ms in the unwrapped sample and 1.51 ms in the Ag-wrapped sample, respectively. This suggested that the enwrapping of Ag nanoparticles had little influence on the f–f inner-shell transitions of Eu^{3+}.

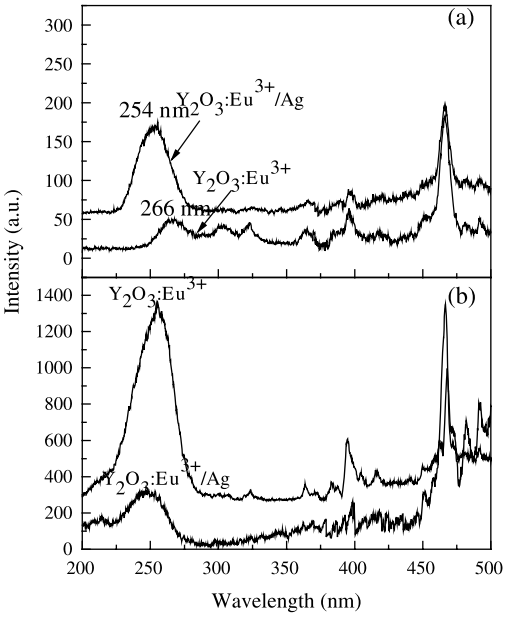

Fig. 4. Excitation spectra of Y_2O_3:Eu^{3+} nanoparticles before and after enwrapped with Ag (a) in glycol (b) in powder (λ_{em}=611 nm).

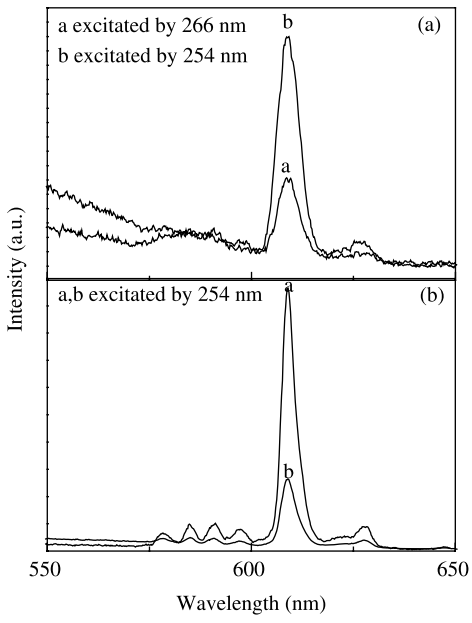

Fig. 5. Emission spectra of the Y_2O_3:Eu^{3+} nanoparticles before (a) and after (b) enwrapped with Ag (a) in glycol and (b) in powder.

The results above suggested that in the glycol solution, the luminescence enhancement for Ag-wrapped sample did not caused by the energy transfer from Ag to Y_2O_3:Eu^{3+} nanoparticles, but caused by the change of surface local environments. In the glycol solution, a large number of vibration modes with large phonon energy such as OH bonds existed. In the un-wrapped Y_2O_3:Eu^{3+} particles, the emissions for the Eu^{3+} ions locating in (or near) the surface were greatly quenched due to nonradiative relaxation from excited state Eu^{3+} ions to some surface bonds. In the Ag-wrapped particles, the thin deposition of Ag in the surface of Y_2O_3:Eu^{3+} formed a protect shell so that the nonradiative relaxation from Eu^{3+} ions to the vibration bonds in the glycol was blocked to some content. As a result, the emission intensity of the $^5D_0$–^7F_J transitions for Eu^{3+} ions increased than that in the un-wrapped particles. Actually, the variation of the location of CT band also originated from the surface local environment change. In the powders, owing to the existence of silvers enwrapped surrounding Y_2O_3:Eu^{3+} particles, a part of excitation light were absorbed or scattered by the surface Ag nanoparticles, leading to the decrease in effective excitation density. As a consequence, the emission intensity of the $^5D_0$–^7F_J transitions for Eu^{3+} in the Ag-wrapped powders decreased. Note that in the solution, the surface absorption and scattering of silver should also happen and lead the emission intensity to decrease. However, in comparison to the influence of nonradiative relaxation from excited state Eu^{3+} ions to surface vibrational bonds in the solution, it is not the key factor.

4. Conclusions

The Ag enwrapped Y_2O_3:Eu^{3+} nanoparticles were prepared in liquid and in powder. The TEM photos demonstrated that the enwrapped Y_2O_3:Eu^{3+} prepared by the combustion method, while the Ag wrapped Y_2O_3:Eu^{3+} well dispersed. In glycol solution, the luminescent intensity of the $^5D_0$–^7F_J transitions for Eu^{3+} for Ag wrapped Y_2O_3:Eu^{3+} increased compared to that for the unwrapped one. This was attributed to the surface local environment change, instead of the energy transfer from Ag to Y_2O_3:Eu^{3+} nanoparticles. In the Ag wrapped Y_2O_3:Eu^{3+} powders, owing to the decrease in effective excitation density the luminescent intensity of the $^5D_0$–^7F_J transitions decreased in comparison to that in the unwrapped one.

Acknowledgements

The author is grateful for the financial support of Nation Natural Science Foundation of China (Grant No. 10374086 and 10504030) and Talent Youth Project of Jilin Province (20040105).

References

[1] J.H. Shin, G.N. van den Hoven, A. Polman, Appl. Phys. Lett. 66 (1995) 2379.
[2] M. Fujii, M. Yoshida, Y. Kanzawa, S. Hayashi, K. Yamamoto, Appl. Phys. Lett. 71 (1997) 1198.
[3] E. Downing, L. Hesselink, J. Ralson, R. MacFarlane, Science (1996) 2721185.
[4] G. Yi, H. Lu, S. Zhao, Y. Ge, W. Yang, D. Chen, L. Guo, Nano Lett. 4 (2004) 2191.
[5] C.M. Niemeyer, Angew. Chem., Int. Ed. 40 (2001) 4128.
[6] W.J. Parak, D. Gerion, T. Pellegrino, D. Zanchet, C. Micheel, S.C. Williams, R. Boudreau, M.A. Le Gros, C.A. Larabell, A.P. Alivisatos, Nanotechnology 14 (2003) R15.
[7] S. Heer, K. Kömpe, H.-U. Güdel, M. Haase, Adv. Mater. 16 (2004) 2102.
[8] J. Hampl, M. Hall, N.A. Mufti, Y.M.M. Yao, D.B. MacQueen, W.H. Wright, D.E. Cooper, Anal. Biochem. 288 (2001) 176.
[9] F. van de Rijke, H. Zijlmans, S. Li, T. Vail, A.K. Raap, R.S. Niedbala, H.J. Tanke, Nat. Biotechnol. 19 (2001) 273.
[10] T. Hayakawa, S.T. Selvan, M. Nogami, J. Non-Cryst. Solids 259 (1999) 16.
[11] T. Hayakawa, S.T. Selvan, M. Nogami, Appl. Phys. Lett. 74 (1999) 1513.
[12] S.T. Selvan, T. Hayakawa, M. Nogami, M. Möller, J. Phys. Chem. B 103 (1999) 7064.
[13] C. Louis, S. Roux, G. Ledoux, L. Lemelle, P. Gillet, O. Tillement, P. Perriat, Adv. Mater. 16 (2004) 2163.
[14] Y. Tao, G. Zhao, W. Zhang, S. Xia, Mater. Res. Bull. 32 (1997) 501.
[15] H. Song, B. Chen, B. Sun, J. Zhang, S. Lu, Chem. Phys. Lett. 372 (2003) 368.
[16] A. Konrad, T. Fries, A. Gahn, F. Kummer, U. Herr, R. Tidecks, K. Samwer, J. Appl. Phys. 86 (1999) 3129.